Environmental Science and Pollution Research (2022) 29:66716–66727
https://doi.org/10.1007/s11356-022-20363-2

RESEARCH ARTICLE

Mitotic and chromosomal effects induced for biosynthesized nanoparticles from three mediators on *Allium cepa* root cells

Nancy Beatriz Andrioli[1,2] · Grace Stephany Solano Mendoza[1] · Jorge Gastón Fernández[3] · María Isabel Sanz Ferramola[3,4]

Received: 5 November 2021 / Accepted: 16 April 2022 / Published online: 4 May 2022

Abstract

The genotoxicity of biogenic silver nanoparticles (AgNPs) obtained from three microbial mediators was assessed using the *Allium cepa* assay. Three clusters were differentiated for the highest frequency of end points of clastogenicity (stick-ends, fragments and bridges), end points of missegregation (C-metaphases and disorder anaphases), and lowest frequency of all the end points. In these clusters, the treatments were grouped respectively as I) positive control (GSF); II) silver nanoparticles form *Aspergillus niger* (AgNPs-An); and III) silver nanoparticles from both *Cryptococcus laurentii* (AgNPs-Cl) and *Rhodotorula glutinis* (AgNPs-Rg), Ag+, and negative control (NC). These results were in according to the principal component analisys (PCA) where treatments were associated to each component of the genotoxic effects. The statistical comparative analysis of the mitotic index (IM) and the abnormal mitosis frequency (AM) indicated that both GSF and AgNPsAn induce significant genotoxic effect. Low genotoxic effects were attributed to AgNPs-Cl and AgNPs-Rg, but mitogenic stimuli, similar to that obtained by the silver ions Ag+, were observed. Results suggested that different features of biogenic nanoparticles such as composition, size, and coating may be involved in the different cytological responses of the meristematic cells.

Keywords Allium cepa · Genotoxicity · Green synthesis · Nanoparticles · Nanotoxicology · Plants toxicology

Introduction

The potential toxic effects of metal nanoparticles (NPs) in general and of the silver nanoparticles (AgNP), in particular on human health and the environment, are continuously reviewed because of their wide use as antibacterial, antiviral and antifungal agents in the agricultural, pharmaceutical, textile, and food industries (Rejeski 2011; Khan et al. 2019). Metal NPs can be obtained through chemical, physical or biological synthesis. In particular, biosynthesis is an efficient method to obtain gold, silver, cadmium sulfide, zinc sulfide, copper, titanium dioxide, zinc oxide and magnetic NPs, among others (Jaidev and Narasimha 2010; Kuppusamy et al. 2016). Moreover, biosynthesis has the advantages of being low cost and environmentally friendly as it does not require the use of toxic reagents. Hence this process is called "green synthesis." Different microorganisms with high nitrate-reductase activity can produce AgNPs by reducing silver ions (Siddiqi et al. 2018). During the biosynthesis process, mediator microorganisms provide nanoparticles (NPs) with capping functional groups that stabilize and functionalize the NPs (Singh et al. 2016; Khoshnamvand et al., 2019; Mohamed et al. 2019). The amphiphilic nature of molecules provides surfactant properties reducing the surface tension and the interfacial energy (Bianchi et al. 2006; Liu et al. 2014). The organic composition of the corona contributes with the high biocompatibility of NPs and prevents the aggregation of NPs. Moreover, it improves movement

Responsible Editor: Gangrong Shi

✉ Nancy Beatriz Andrioli
nancyandrioli@gmail.com

[1] GIBE (Grupo de Investigación en Biología Evolutiva), FCEyN-UBA, Facultad de Ciencias Exactas Y Naturales. Ciudad Universitaria, Pabellón II, 4° Piso Laboratories. 43-46, C1428EGA Buenos Aires, Argentina

[2] Instituto de Ecología, Genética y Evolución de Buenos Aires (IEGEBA−CONICET), Ciudad Universitaria, Pabellón II, 4° Piso Laboratories. 43-46, C1428EGA Buenos Aires, Argentina

[3] Facultad de Química, Bioquímica y Farmacia, Universidad Nacional de San Luis, San Luis, Argentina

[4] INQUISAL-CONICET-UNSL, Ejército de Los Andes 950, D5700HHW San Luis, Argentina

into the cellular compartments and retention of the biogenic particles inside the organisms to interact with other biomolecules (Deepak & Kalishwaralal, 2011; Mohanta et al. 2018; Akther et al. 2019). In this regard, diverse functional groups have been reported to improve the potential applications of AgNPs (Durán et al. 2011; Ortega et al. 2015). Thus, the incorporation of polymers and surfactants to the NP surface as additional step required in chemical manufacture of NPs to their functionalization is not necessary in the biogenesis.

In fungi, electrostatic interactions between the Ag + ions and negative charges of proteins of the cell wall of fungus seem to be involved in the biogenesis of metallic NPs with electron transfer by NADH and NADH-dependent nitrate reductase enzymes. Biomolecules such as polysaccharides and proteins are incorporated as capping agents simultaneously with biogenesis processes from the fungal exudates (Baymiller et al., 2017; Gudikandula et al., 2017; Mukherjee et al., 2001). The different features of NPs, such as chemical coating, diameter, surface charge and degree of aggregation depend on the synthesis method and play an important role in their interaction with cells (Kandlikar et al. 2007; Schrand et al. 2010; Dietz and Herth 2011; Metz et al. 2015; Jeevanandam et al. 2018; Jorge de Souza et al. 2019).

Regardless of the the synthesis method most AgNPs toxicity studies have focused on, the role of ions released from nanoparticles in cytotoxic induction, the effect of nanoparticle size on cytotoxicity, the dose–response relationship and the mechanism of uptake and subsequent distribution in tissues and cells (Beer et al., 2012; Park et al., 2011; R. P. Singh & Ramarao, 2012). In addition to oxidative stress, which is the most important mechanism attributed to surface interaction between AgNPs and cells, the presence of a chemical coating may also be involved in other interactions promoting cytotoxic and genotoxic responses (Donaldson et al. 2010; Gonzalez et al. 2017; Karami and De Lima 2016). So far, toxicological studies of NPs have used different biological models (Park et al. 2011; Beer et al. 2012; Ghosh Chaudhuri and Paria, 2012; Bahadar et al. 2016). Particularly in plants, toxicological effects have been reported for germination, photosynthesis, growth, and development, while cytotoxic and genotoxic effects have been scarcely explored (Karami and De Lima 2016; Scherer et al. 2019). Several genotoxicity and cytotoxicity studies of NPs have used *Allium cepa* or *Allium sativum* to evaluate commercial NPs and the most common abnormalities found in mitosis were fragments, C-metaphases, anaphasic bridges, sticky ends and disorganized anaphases (Kumari et al. 2009, 2011; Babu and Sabesan 2012; Shaymurat et al. 2012; Nagaonkar et al. 2015; Raskar and Laware 2014). Nuclear abnormalities and micronucleus have also been documented (Shaymurat et al., 2012; Pakrashi et al., 2014; Scherer et al., 2019).

Allium cepa is a plant model widely used in toxicity, cytotoxicity, and genotoxicity studies which proved to be appropriate for the analysis of root growth, proliferation of meristematic cells, chromosomal damage, microtubule array disruption, and oxidative injury (Leme and Marin-Morales 2009; Andrioli and Mudry 2011; Andrioli et al. 2012, 2014). The *Allium cepa* aberration bioassay is validated by the International Programme on Chemical Safety (IPCS, WHO) and the United Nations Environment Programme (UNEP) as a standard test of environmental genotoxicity induced by chemical substances (Fiskesjö, 1985; Grant, 1982). In the present study, the AgNPs biosynthesized from the mediator microorganisms *Cryptococcus laurentii* (BNM 0525), *Rhodotorula glutinis* (BNM 0524) and *Aspergillus niger (*NRRL 1419) were evaluated for genotoxic potential employing standard *Allium cepa* assay. Early studies on these materials in our laboratory showed that water filters containing AgNPs from *R. glutinis* or *C. laurentii* were more effective as antimicrobial agents than filters with AgNPs from *A. niger* (Fernández et al., 2015). Since the AgNPs from *C. laurentii* and *A. niger* are about twice higher than *R. glutinis*, this result was not expected for the surface charge effect. In addition, the FTIR spectroscopy to investigate the chemical nature of the compounds involved in the stabilization of nanoparticles showed that in AgNPs from *A.niger* these compounds are rich in proteins, whereas in *R. glutinis* and *C. laurentii*-mediated AgNPs the carbohydrates are more predominant compounds (Fernández et al., 2015, 2016). Furthermore, in the same assay, the adhesion of biogenic AgNPs to filters suggested that the functional groups of the capping agents interact with molecules of nitrocellulose.

Therefore, these results lead to question whether different genotoxic potential of AgNPs biosynthesized from the mediator microorganisms also could be observed in the *Allium cepa* cytotoxicity and genotoxicity assay. For this goal, the meristematic cells of *Allium cepa* were exposed to AgNPs at two exposure times: during less than one mitosis cycle (short-term exposure) and more than one mitosis cycle (long-term exposure) to compare their respective responses. The genotoxic effects were limited to quantification of abnormalities observed during mitosis at both exposure times. Nuclear abnormalities observed in interphase were not quantified to avoid redundancy, as they result from the damage occurring in the previous mitosis (Fernandes et al., 2007; Fenech et al., 2011). We discuss the relationship between the response of the meristematic cells and the features of the biosynthesized AgNPs to provide insight into potential applications and to evaluate exposure hazard of cells to these AgNPs.

Materials and methods

Origin and characteristics of biosynthesized AgNPs

The AgNPs were obtained and characterized by the Industrial Microbiology Laboratory, Universidad Nacional de

San Luis, Argentina. The microorganisms used as mediators for the synthesis of AgNPs were *Aspergillus niger* (NRRL 1419), *Cryptococcus laurentii* (BNM 0525) and *Rhodotorula glutinis* (BNM 0524). The applied synthesis methods and characterization were performed as described in Fernandez et al., 2016 (Fernández et al., 2015, 2016). AgNP characterization included average size and chemical composition of the capping. Assays of the functional groups conjugated with the surface of AgNPs and Fourier transformed infrared studies (unpublished data), confirmed the presence of yeast proteins and polymeric carbohydrates surrounding this nanoparticle. The biosynthesized AgNPs from *A. niger* (AgNPs-An) had a size of 40 ± 5 nm and showed a high concentration of proteins and a low concentration of carbohydrates. The sizes of AgNPs from *C. laurentii* (AgNPs-Cl) and *R. glutinis* (AgNPs-Rg) were 35 ± 10 and 15 ± 8 nm, respectively. A high concentration of arabinogalactan-type polysaccharides and a low concentration of proteins surrounded the AgNPs-Cl, whereas a high concentration of carbohydrates of the arabinan and galactoglucomannan types surrounded the AgNPs-Rg.

Preparation of samples

The AgNPs concentration was determined in culture supernatant from yeasts by UV–visible spectrophotometry at 420 nm. A potentiostat 172 PGSTAT 302 N, AUTOLAB having a value of 0,001 mg.L -1, was used to measure the potentiometry of the residual silver ion concentration The AgNPs samples of known concentrations were sonicated for 3 cycles of 10 s each with cooling intervals. The dilutions of the biosynthesized AgNPs were prepared at a concentration of 1 ug/ml. Dechlorinated water was used as negative control (NC), griseofulvin (GSF, Sigma, CAS No.126–07-8) at 200 ug/ml GSF as chemical positive control and 1 ug/ml silver nitrate salt solution (Ag +) was included as reference of the cytotoxic and the genotoxic response to the ions exposure.

Exposure of bulbs

Bulbs of *Allium cepa* (cv. Valcatorce INTA) of about 3–5 cm in diameter were placed in containers with dechlorinated water for 24 h until roots reached about 2 mm in length. Then, bulbs were exposed to different treatments under constant bubbling (three replicates each). Taking into account that the duration of the mitotic cycle in root meristematic cells is 13–15 h (N. Andrioli, 2011; Campo et al., 2003), we selected two different exposure times. Thus, roots were exposed to AgNPs and controls for 4 h (short-term exposure) and 30 h (long-term exposure).

After exposure, roots were fixed in a 3:1 ethanol-acetic acid solution for 24 h and then kept in 70% ethanol until examination under a Leica DMLB light microscope (1000 ×).

Data exploration and statistical analysis

Exploratory and statistical analyses were performed using RStudio 3.3.6. The end points measured in the short- and long-term exposure assays were number of cells in each phase, namely, interphase, prophase, metaphase, anaphase and telophase. The mitotic abnormalities quantified were disorganized anaphases and C-metaphases, sticky-ends, bridges and fragments (Fig. 1a–f). About 1000 cells were scored per replicate. Other variables for descriptive analysis derived from the measured endpoints were mitotic index (MI), calculated as the number of cells in mitosis/total number of cells observed; and frequency of abnormal mitosis (AM), calculated as the number of cells with abnormal mitosis/total number of cells in mitosis.

The exploratory data analysis was conducted to determine the distribution of the response variables MI and AM according to the different explanatory variables. To assess if the grouping of mitotic abnormalities were influenced by treatment and exposure time, either separately or combined, we conducted a cluster analysis (CA) using the non-hierarchical k-means method with the cluster package in R studio. In order to determine the optimal number of clusters, the NbClust package was applied. It is based on 30 indices obtained by all combinations of number of clusters, distance measures, and clustering methods (Charrad et al., 2014).

A multivariate analysis principal component analysis (PCA) was performed to reduce the number of variables indicators of mitotic abnormalities, obtaining a set of new variables as a linear combination of the original variables which characterize the genotoxic damage. In addition to the kaiser criterion, the cumulative variability explained by principal components and the sedimentation plot was used as criteria for choosing the number of principal components. Each principal component allowed to characterize the effect according to the magnitude and sign of the eigenvector loading. The measure of the angle in the biplot indicates the correlation between abnormalities. Values were scaled and centered so that the type and intensity of effect is determined by their location in the quadrants and distance to the center (i.e., average value).

ANOVA was used to test for differences in mitotic abnormalities and mitotic index between AgNP treatments and controls obtained from the principal components. The non-parametric Kruskal–Wallis test was used if variables did not meet normality and homoscedasticity assumptions. Comparisons between treatments and their negative controls were conducted using post hoc tests. Significance levels were set at p-values < 0.05; p-values between 0.1 and 0.05 were considered as slighly significant.

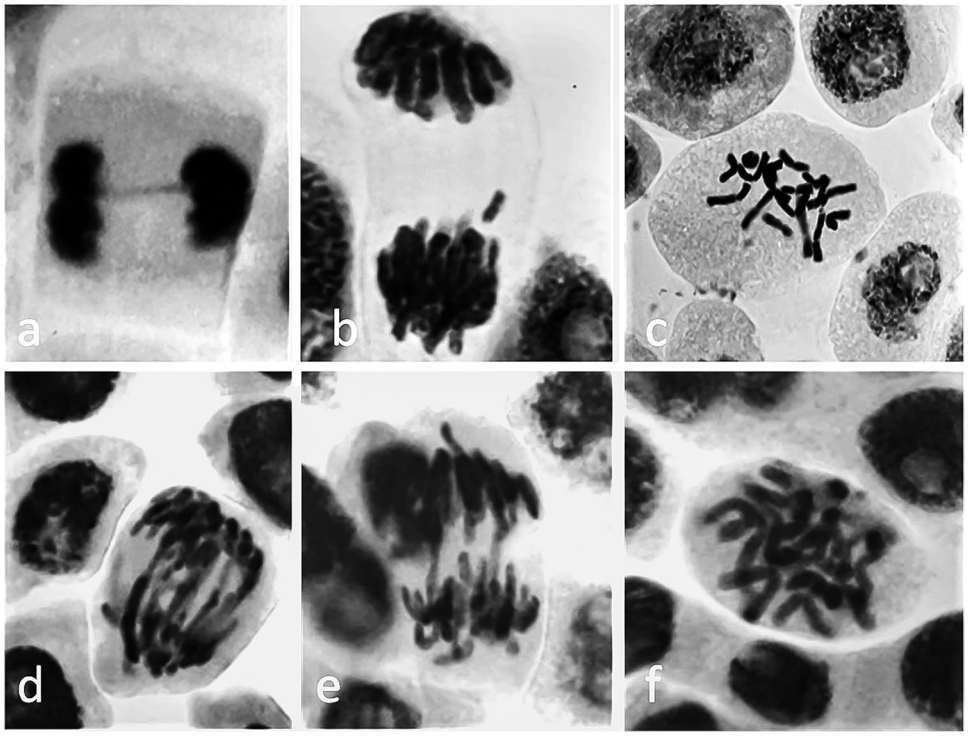

Fig. 1 **a)** Bridge, **b)** Fragments, **c** and **f)** C-metaphases, **d)** Disorganized anaphases, **e)** Sticky-ends

A generalized linear mixed model (GLMM) was performed to evaluate the association between each explanatory feature (treatment and exposure time) and the response variables, also considering the interactions between explanatory variables. The independent variables used in the analysis were: treatment, AgNPs-An, AgNPs-Cl, AgNPs-Rg, Ag+, NC, and GSF as factors; exposure time was treated as a binary variable scored 0 (short-term exposure) and 1 (long-term exposure). The replicates were included as random factors to control overdispersion (Harrison, 2014). For MI and AM, we assumed a binomial distribution of errors and applied the Logit function as a link for the response variables using the glmer function of the lme4 R-package(Bates et al., 2014). The final model was chosen, according to their lower Akaike Information Criteria (AIC).

Results

Exploratory analysis

The distribution of the values of MI and AM, arranged per treatment and exposure time, is represented with a box-plot. No outlier values were detected according to the interquartile ratio. For both time exposures, the mitotic depletion is observed to GSF and AgNP-An exposure more than to AgNPs-Cl, AgNPs-Rg, Ag+compared with the NC. Moreover, the exposure to AgNPs-Cl and Ag+yielded higher mitosis values than did the NC (Fig. 2a–b). The inverse results obtained for the AM values suggest that the arrest of the cell cycle is a result of genotoxicity damage (Fig. 2c–d).

Cluster analysis

From the frequency of the end points, the cluster analysis was performed. Three clusters were the optimal number obtained in according to the majority rule from different methods. The treatment and time exposure labels into the groups suggested the existence of interactions between both factors (Fig. 3a). Thus, a cluster analysis was performed with the data from each exposure time separately. Five and three clusters were the optimal number respectively, at short and long-term exposure, respectively. The comparison of results showed that clusters were formed according to the treatment only for the long-term exposure as follows: I) GSF; II) AgNPs-An; and III) NC, AgNPs-Cl and AgNPs-Rg, Ag+(Fig. 3b–c).

Principal component analysis (PCA)

Table 1 presents the results of the PCA analysis which transforms the variables (mitosis abnormalities) to PCs by linear combination. Hence, the dimension was reduced from five original variables to three components which explain the 86% of the variance. This number of PCs was estimated based on both Kaiser criterion as well as the amount of explained variance. Absolute values greater than 0.5 were considered for the genotoxicity characterization of PCs. PC1

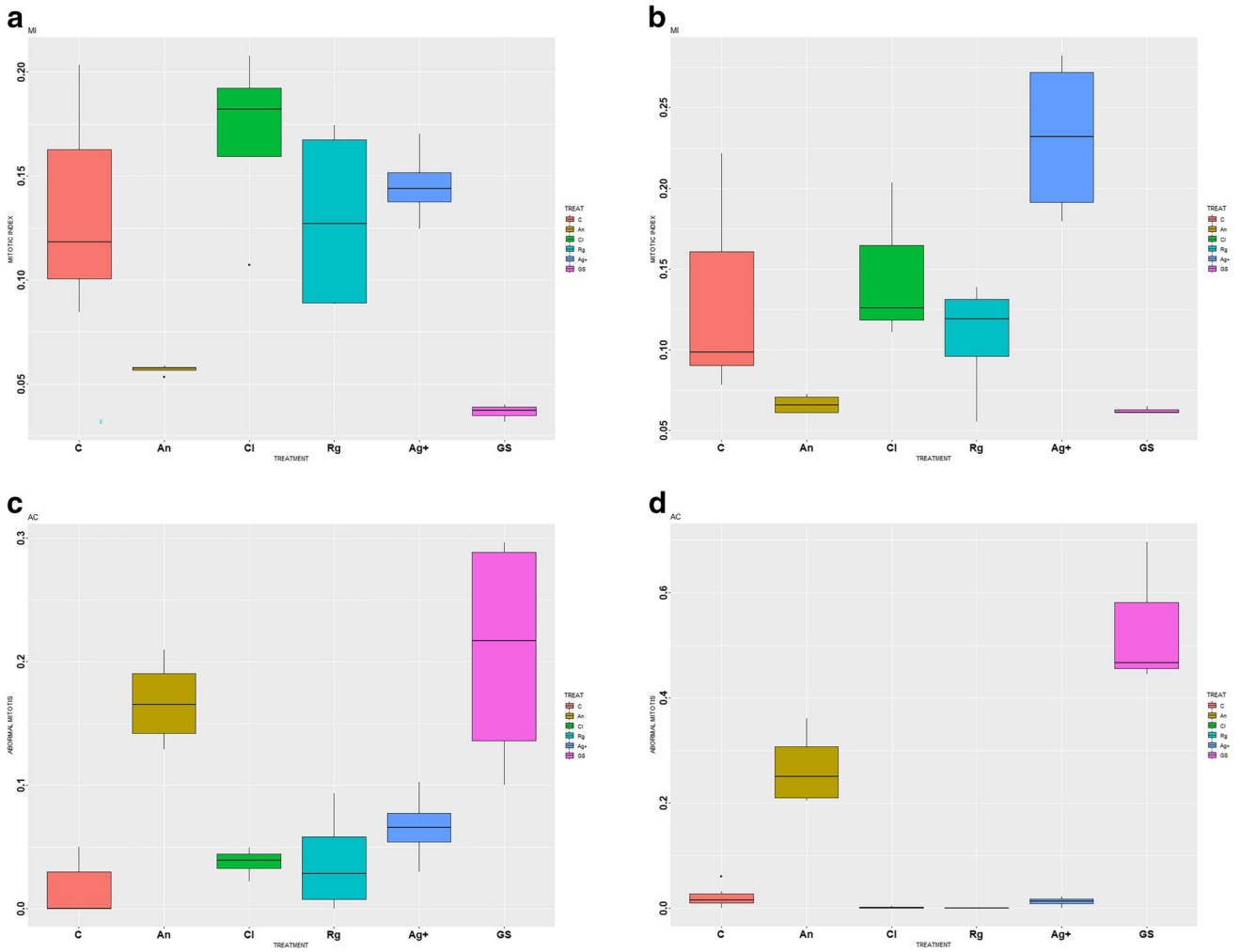

Fig. 2 **a–b)** Boxplot showing the distribution of Mitotic index values per treatment arranged according to exposure time. a: short-term exposure; b: long-term exposure. **b–c)** Boxplot showing the distribution of Abnormal mitosis frequency values per treatment arranged according to exposure time. b: short-term exposure; d: long-term exposure. An = treatment with nanoparticles biosynthesized from *Aspergillus niger*, Cl = treatment with nanoparticles biosynthesized from *Cryptococcus laurentii*, Rg = treatment with nanoparticles biosynthesized from *Rhodotorula glutinis,* NC = Negative control, Ag + : Silver Nitrate salt, GSF = Griseofulvin (Positive control)

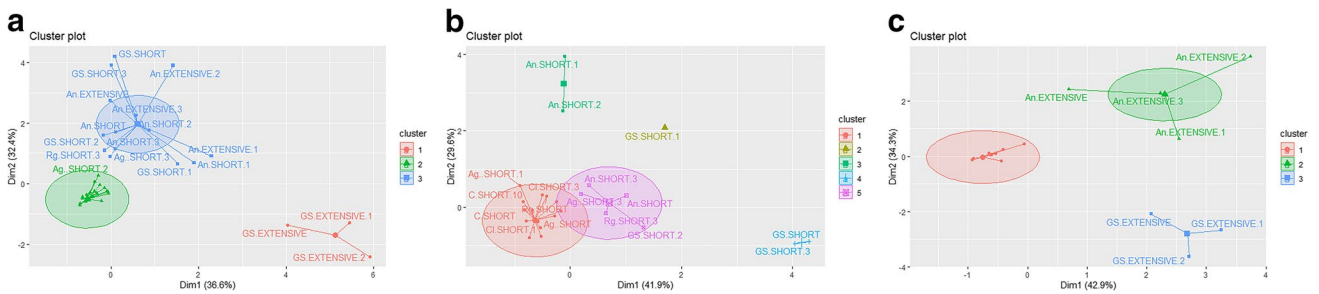

Fig. 3 Clusters of mitotic abnormalities obtained by the k-means. **a)** Labels inside clusters indicate the treatments and exposure time. **b)** Treatment and concentration at short-term exposure. **c)** Treatment at long-term exposure. An = treatment with nanoparticles biosynthesized from *Aspergillus niger*, Cl = treatment with nanoparticles biosynthesized from *Cryptococcus laurentii*, Rg = treatment with nanoparticles biosynthesized from *Rhodotorula glutinis,* NC = Negative control, Ag + : Silver Nitrate salt, GSF = Griseofulvin (Positive control)

Table 1 Principal components obtained from mitotic abnormalities used as endpoints. The values correspond to loads of the factors obtained from the linear combination of the original variables e indicate to the correlations between PC and mitotic abnormalities

	PC1	PC2	PC3	PC4	PC5
STICKY-ENDS	0.56125	-0.41413	0.22049	0.04109	-0.68058
FRAGMENT	-0.02660	0.34198	0.90368	0.24435	0.07749
DISORGANIZED ANAPHASES	0.37315	0.52606	-0.36099	0.66766	0.08902
C-METAPHASES	0.29789	0.62544	-0.02370	-0.69672	-0.18466
BRIDGES	0.67551	-0.20886	0.06225	-0.08610	0.69913

PC principal component

is a component of clastogenicity because it is positive and correlates with the sticky-ends and bridge end-points. PC2 is a component of segregational disturbance because it is positive and correlates with the disorganized anaphases and C-metaphases. Finally, PC3 is a component of clastogenicity which correlates positively and strongly with fragments (Table 1).

The biplots show that correlations are stronger between C-metaphases and disorganized anaphases, and between bridges and sticky-ends, than between all four end points and fragments. Moreover, the GSF and AgNPs-An were associated with the segregation component, GSF was associated with clastogenic damage, and the NC and AgNPs-Rg, Ag + and AgNPs-Cl were associated with low genotoxic effects (Fig. 4(a–b)).

GLMM and comparative statistical analisys

Treatment and exposure time

The influence of treatments and exposure time on the mitosis frequency and the induction of abnormal mitosis was analyzed with GLMM. The occurrence of mitosis was negatively and significantly associated with AgNPs-An and GSF. The long-term relative to short-term exposure were not significatively associated with the global response, but their interaction with AgNPs-An, Ag + or GSF were positive and significantly associated with mitosis frequency (Table 2). Since the interaction coefficient between treatment and exposure time was significant, the comparative analyses were performed separately for short and long-term. In according to GLMM, the multiple comparisons between treatments at short-term showed significant differences in MI for GSF and AgNPs-An with respect to the NC. At long-term, only Ag + were positive and significantly different from the NC. In addition, the significant differences between treatments is evidence of their different cytotoxicity potential (Table 3).

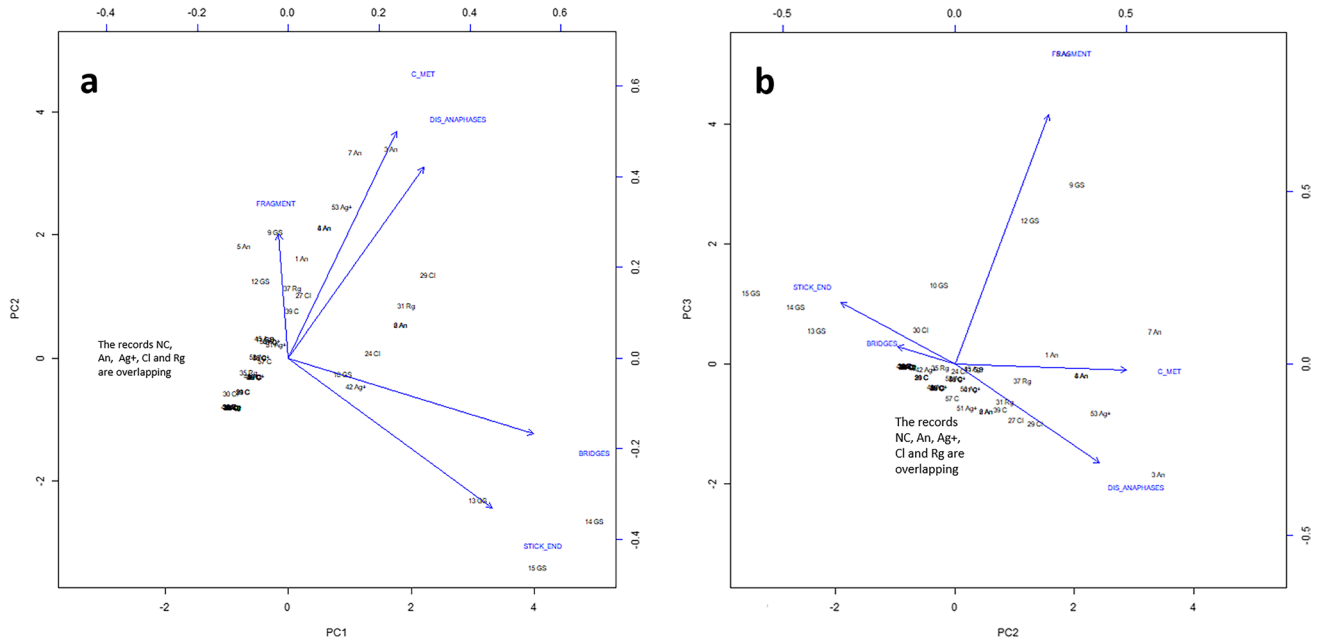

Fig. 4 Principal components (PCs) for mitotic abnormalities. Biplot performed with mean values of mitotic abnormalities per treatment **a)** PC1 and PC2 **b)** PC2 and PC3. An = treatment with nanoparticles biosynthesized from *Aspergillus niger*, Cl = treatment with nanoparticles biosynthesized from *Cryptococcus laurentii,* Rg = treatment with nanoparticles biosynthesized from *Rhodotorula glutinis,* NC = Negative control, Ag + : Silver Nitrate salt, GSF = Griseofulvin (Positive control)

Table 2 Association of independent variables treatments and time exposure with mitosis frequency

Variables	Coefficients	Pr(>|z|)
(Intercept)	1.86855	$<2e\text{-}^{16}$***
AgNPsAn	-1.41373	$<2e\text{-}^{16}$***
AgNPsCl	0.10356	0.46311
AgNPsRg	-0.11699	0.10916
Ag +	-0.01369	0.87287
GSF	-1.78712	$<2e\text{-}^{16}$***
Long term	-0.16942	0.19549
AgNPsAn: Long term	0.80824	0.00184**
AgNPsCl: Long term	0.26862	0.09541
AgNPsRg: Long term	0.04372	0.77737
Ag + : Long term	0.77558	9.05 e-06***
GSF: Long term	0.17992	3.61e-09***

Signif. Level '***' $p<0.001$, $p<$ '**' 0.01, $p<$ '*' 0.05. The coefficients corresponding to the treatment levels are relative to the negative control and those of the exposure time levels are relative to the shot term exposure

Table 3 Multiple comparisons and post hoc test contrasts between treatments and negative control for mitosis frequency

Test	*Exposure*	*p-value*	Post hoc contrasts	*p-value*
Kuskal-Wallis	Short	0.0016**	AgNPsAn—NC	0.005**
			Ag + —AgNPsAn	0.005**
			AgNPsCl—AgNPsAn	0.015*
			GSF – NC	0.017*
			AgNPsCl – GSF	0.0069**
			Ag + -GSF	0.098
			GSF—AgNPsRg	0.053*
Kuskal-Wallis	Long	0.0026**	AgNPsAn—NC	0.084
			GSF-NC	0.07
			AgNPsRg-NC	0.092
			Ag + – AgNPsAn	0.072
			GSF – AgNPsRg	0.008**
			AgNPsAn – AgNPsRg	0.007**
			AgNPsAn – AgNPsCl	0.07
			Ag + -NC	0.005**
			Ag + —AgNPsRg	0.09

Signif. Level '***' $p<0.001$, '**' $p<0.01$, '*' $p<0.05$

AgNPs-An treatment with nanoparticles biosynthesized from *Aspergillus niger*, *AgNPs-Cl* treatment with nanoparticles biosynthesized from *Cryptococcus laurentii*, *AgNPs-Rg* treatment with nanoparticles biosynthesized from *Rhodotorula glutinis, NC* negative control, *GSF* Griseofulvin (Positive control), Ag + : Silver Nitrate salt. (The NC and Short-term exposure are the reference factors in generalized linear mixed model)

Significant associations were found in the treatments, being the higher positive association with abnormal mitosis AgNPs-An and GSF treatments, while the AgNPs-Cl, AgNPs-Rg and Ag + treatments showed a weak association (Table 4). Results of these analyses showed significant differences for AM between NC and GSF and between NC and AgNPs-An at short-term exposure. Significant differences for AM between NC and GSF were observed at long-term exposure. In addition, significant differences in the genotoxicity potential are observed between other treatments. (Table 5).

Table 6 is presented to compare the PCs among both the treatments and the exposure times. Significant differences between the treatments and NC to each PC1 and PC2 at the short-term exposure and each PC1, PC2, and PC3 at the long-term exposure suggested that GSF and AgNPs-An induce differential genotoxicity damage, being AgNPs-An only associated to the segregational disruption component PC2, whereas GSF is associated also to clastogenic component PC1 and PC3. (Table 6).

Discussion

The biosynthesis of nanoparticles (NPs) has many environmental advantages and is widely used in the pharmaceutical, agricultural, textile and food industries. This emphasizes the need for the assessment of potential human health and environmental hazard. In this study, we used the *Allium cepa* assay, and characterized some endpoints to gain insight into the genotoxicity potential of AgNPs obtained from three different microbial mediators. The genotoxicity damage can

Table 4 Association of variables, treatments, and exposure times with abnormal mitosis

Variables	Coefficients	Pr(>|z|)
(Intercept)	-5.49626	$<2e\text{-}^{16}$***
AgNPs-An	3.16468	$<2e\text{-}^{16}$***
AgNPs-Cl	1.31894	0.000973***
AgNPs-Rg	1.12155	0.011288*
Ag +	1.54501	0.000191***
GSF	3.48135	$<2e\text{-}^{16}$***
Long term	0.45623	0.260697
AgNPs-An: Long term	-0.05581	0.906577
AgNPs-Cl: Long term	-3.61129	0.001045**
AgNPs-Rg: Long term	-28.02873	0.956343
Ag + : Long term	-1.78383	0.003279**
GSF: Long term	0.19039	0.703968

Signif. Level: '***' $p<0.001$, '**' $p<0.01$, '*' $p<0.05$. The coefficients corresponding to the treatments levels are relative to the negative control and those of the exposure time levels are relative to the shot term

Table 5 Multiple comparisons and post hoc test contrasts between treatments and negative control for abnormal mitosis frequency

Test	*Exposure*	*p-value*	Post hoc contrasts	*p-value*
Kuskal-Wallis	Short	0.00058	AgNPsAn—NC	0.003*
			Ag + -NC	0.090
			AgNPsCl—NC	0.43
			GSF – NC	0.0035**
			AgNPsCl – GS	0.093
			GS—AgNPsRg	0.098
Kuskal-Wallis	Long	0.00076	AgNPsAn—NC	0.077
			Ag + -NC	0.71
			AgNPsCl -NC	0.25
			GSF-NC	0.036*
			AgNPsRg-NC	0.092
			Ag + – AgNPsAn	0.072
			GS – AgNPsRg	0.005**
			AgNPsAn—AgNPsRg	0.007**

Signif. Levels: '**' $p < 0.01$ '*' $p < 0.05$; '·' $p < 0.1$

be due to the direct interaction with DNA leading to chromatin breaks, or indirect interation with components of the mitotic machinery as the microtubule and associate proteins (MAPs) which are involved in segregation of chromatids. Both kinds of damage are named as clastogenic or aneugenic effects respectively (Kirsch-Volders et al., 2003; Mishima, 2017). These effects can be inferred through the abnormalities of the mitosis in the standardized *Allium cepa* assay whereas the mitotic index and phase index indicate the cellular proliferation disturbances. The uptake and impact of NPs on biological systems depend on several factors such as their molecular composition, aggregation, quantity and size. The chemical composition and surface area contribute to reactivity, while size facilitates their uptake into tissues (Gonzalez et al. 2017; Ortega et al. 2015). In addition, the interactions between NPs and biomolecules could be conditioned by the biology of cells such as the metabolic rate, redox potential, and antioxidative system, among others (Asharani et al., 2008). In plants, NPs are distributed and translocated by vessels (Zhu et al., 2008). The NPs with sizes of up to 20 nm can pass through cell wall pores and move between cells via plasmodesmata or are taken up by endocytosis (Ma et al., 2010). Once inside the cell, free metal ions may induce redox imbalance and oxidative damage (Carlson et al., 2008; R. P. Singh & Ramarao, 2012). Scherer et al. (2019), who studied the effect of commercial AgNPs coated with the neutral polymer PVP (AgNPs-PVP) on *Allium cepa* meristematic root cells, reported that these were very stable in aqueous solution and released low levels of Ag + ; indicating that they were mainly responsible for

Table 6 Multiple comparisons and post hoc test contrasts among treatments and negative control for principal component from abnormal mitosis

Test	*Component*	*Exposure*	*p-value*	Post hoc contrasts	*p-value*
Kuskal-Wallis	PC1	Short	0.0042**	AgNPsCl-NC	0.029*
				AgNPsAn-NC	0.009**
ANOVA	PC2	Short	0.0009***	AgNPsAn-NC	< 0.001***
				Ag + -NC	0.0390*
				GSF-NC	0.0199*
				AgNPsRg -AgNPsAn	0.0428*
Kuskal-Wallis	PC3	Short	0.015**	Ag + – GSF	0.024*
				AgNPsCl—GSF	0.045*
Kuskal-Wallis	PC1	Long	0.001***	NC – GSF	0.029*
				AgNPsRg -AgNPsAn	0.028*
				GSF -AgNPsRg	0.0047**
Kuskal-Wallis	PC2	Long	0.0009***	AgNPsAn—NC	0.07
				AgNPsAn – AgNPsCl	0.024*
				Ag + – GS	0.042*
				AgNPsAn – GS	0.0009***
				NC—GSF	0.028*
				AgNPsAn—AgNPsRg	0.0089 **
Kuskal-Wallis	PC3	Long	0.014*	GSF—NC	0.019*

Signif. Levels: '**'0.01 '*' 0.05; '·' 0.1 '

a–c: AgNPs-An = treatment with nanoparticles biosynthesized from *Aspergillus niger*, AgNPs-Cl = treatment with nanoparticles biosynthesized from *Cryptococcus laurentii*, AgNPs-Rg = treatment with nanoparticles biosynthesized from *Rhodotorula glutinis,* NC = Negative control, GSF = Griseofulvin (Positive control), Ag + : Silver Nitrate salt (The NC and Short term exposure are the reference factors in generalized linear mixed model)

the cytotoxicity and genotoxicity of AgNPs-PVP. Moreover, this same study showed that AgNPs ranging between 10 and 73 nm were able to enter the roots, and the authors attributed the genotoxic and cytotoxic effects to a higher surface area of contact and higher reactivity of the smaller nanoparticles. The inverse relationship between NP cytotoxicity and size has also been reported for other biological models (Feizi et al., 2013; Gao et al., 2015). This is in disagreement with our results, which showed that the largest-sized AgNPs used in the present study, namely AgNPs-An, induced a higher abnormal mitosis frequency than did AgNPs-Cl and AgNPs-Rg, suggesting that the genotoxicity potential could be attributed to other distinctive features, such as the functional groups of coating. The results obtained from the comparison of principal components between treatments showed differential association between clastogenicity and GSF and between segregational disruption and AgNPsAn, in acording to the cluster analysis which grouped separately both treatments based in the end points. The cluster analysis showed that data were grouped in according to treatments at the long term-exposure but not at the short-term exposure. This may reveal that cells require passing through more than one mitosis cycle to express the deleterious effect of treatments. Differential effects were founded in the statistical comparative analysis of PCs where significant differences between AgNPs-An and NC were only at short-term exposure for the PC1 and PC2, indicating clastogenic effects associated to stick ends and bridges and the segregational disturbance respectively. Finally, at long-term exposure the positive control GSF is the only treatment which showed significan differences with the NC for the three PCs. In this regard, early studies suggested that the GSF interaction with the microtubules associated molecules (MAPs) lead to multiple genotoxic effects (Andrioli et al., 2014). The MI values were higher in cells exposed to AgNPs-Cl and Ag + than to the NC. Such effect could be explained by an increase in reactive oxygen species (ROS) due to the interaction of Ag + with *A. cepa* meristems, activating signals that modulate the regulation of cellular proliferation, as previously reported for other proliferative tissues (Laurent et al., 2005). This mechanism may be considered a secondary effect of the ROS, which paradoxically, provokes cellular arrest or apoptosis at high concentrations and proliferation at low levels (Boonstra and Post 2004; Laurent et al. 2005). Interestingly, AgNPs-Cl has been reported to induce apoptosis in tumor cells at a concentracion five times higher than the one used here (Ortega et al., 2015). Moreover, in a recent study, Heikal et al., (2020) found higher values of MI, compared to the negative control, in *Allium cepa* meristematic root cells exposed to biogenic AgNPs, and the authors attributing these result to the antioxidant response.

In this study, the effects observed in the meristematic cells suggest that the different features of biosynthesized AgNPs such as functional groups of the coating could influence these mitotic responses. Several studies indicate that the protein surrounding the NPs could facilitate the dispersion and translocation into the compartimentalization of the cells and interact with microtubules, protein kinases, topoisomerases, centrosomes and kinetochores, etc. (Donaldson et al., 2010). The study of the interaction between NPs and cells requires a broader perspective about the process involved in comparison to those between the cells and chemical structures, such as GSF. Indeed, different authors call for a change in the paradigm of genotoxic evaluation of nanomaterials (Donaldson et al., 2010; Gonzalez et al., 2017). Studies focused on the molecular changes into the cells could increase the knowledge of the influence of the different features of NPs on multiple interactions and cellular targets and contribute to predict important cellular responses. However, more studies will be necessary to know the nature of the interactions.

Conclusion

The AgNPs could interact with cellular targets which included DNA and other molecular components involved in mitosis. Our study allowed evidence that the biosinthesized AgNPs-An which have protein as functional group prevalent in the surrounding, to differentiate the other biogenic AgNPs studied, induce genotoxicity by segregational disruption. These insights would allow to improve exposure hazard evaluation of biosynthesized metal NPs as well as to expand the scope of research on the beneficial biological applications of the green synthesis.

Supplementary Information The online version contains supplementary material available at https://doi.org/10.1007/s11356-022-20363-2.

Author contribution Nancy B. Andrioli**:** Conceptualization, Investigation, Software, Writing-Reviewing and Editing, Visualization. Stephany Solano Mendoza: Investigation, methodology. Jorge G Fernandez*:* Resources, Investigation. María I Sanz Ferramola: Resources, Supervision, Funding acquisition, Writing-Reviewing and Editing.

Funding This work is financially supported by the Universidad de Buenos Aires, Argentina (grant UBACyT 20020170200367BA) and by the Universidad Nacional de San Luis, Argentina (grant PRICO 02–2716).

Data availability All data generated or analysed during this study are included in this published article and its supplementary information files.

Declarations

Ethics approval (Not applicable).

Consent to participate (Not applicable).

Consent for publication (Not applicable).

Competing interests The authors declare no competing interests.

References

Akther T, Mathipi V, Kumar NS, Davoodbasha M, Srinivasan H (2019) Fungal-mediated synthesis of pharmaceutically active silver nanoparticles and anticancer property against A549 cells through apoptosis. Environ Sci Pollut Res 26(13):13649–13657. https://doi.org/10.1007/s11356-019-04718-w

Andrioli N (2011) Evaluación de agentes químicos con potencial genotóxico en células meristemáticas de Allium cepa. Tesis Doctoral 41–49

Andrioli NB, Mudry MD (2011) Cytological and cytogenetic effects induced by thiabendazole on Allium cepa root meristems. BAG - J Basic Appl Genet 22(2):17–23

Andrioli NB, Soloneski S, Larramendy ML, Mudry MD (2012) Cytogenetic and microtubule array effects of the zineb-containing commercial fungicide formulation Azzurro ® on meristematic root cells of Allium cepa L. Mutat Res Genet Toxicol Environ Mutagen 742(1–2):48–53. https://doi.org/10.1016/j.mrgentox.2011.11.014

Andrioli NB, Soloneski S, Larramendy ML, Mudry MD (2014) Induction of microtubule damage in Allium cepa meristematic cells by pharmaceutical formulations of thiabendazole and griseofulvin. Mutat Res Genet Toxicol Environ Mutagen 772:1–5. https://doi.org/10.1016/j.mrgentox.2014.06.009

Asharani PV, Wu YL, Gong Z, Valiyaveettil S (2008) Toxicity of silver nanoparticles in zebrafish models. 255102. https://doi.org/10.1088/0957-4484/19/25/255102

Babu K, Sabesan G (2012) Effect of Nano-Silver on Cell Division and Mitotic Chromosomes: A Prefatory Siren. Int J Nanotechnol 2(2). https://doi.org/10.5580/10eb

Bahadar H, Maqbool F, Niaz K, Abdollahi M (2016) Toxicity of nanoparticles and an overview of current experimental models. Iran Biomed J 20(1):1–11. https://doi.org/10.7508/ibj.2016.01.001

Bates D, Maechler M, Bolker B, Walker S, Chistensen (2014) Linear mixed-effects models using "Eigen" and S4.

Baymiller M, Huang F, Rogelj S (2017) Rapid one-step synthesis of gold nanoparticles using the ubiquitous coenzyme NADH. Matters 8–11 https://doi.org/10.19185/matters.201705000007

Beer C, Foldbjerg R, Hayashi Y, Sutherland DS, Autrup H (2012) Toxicity of silver nanoparticles-Nanoparticle or silver ion? Toxicol Lett 208(3):286–292. https://doi.org/10.1016/j.toxlet.2011.11.002

Bianchi CL, Ardizzone S, Capperelletti G (2006) Nanocrystalline Oxides : Surfactants-Assisted Growth. Encyclopedia Nanosci Nanotechnol January 1–10. https://doi.org/10.1081/E-ENN-120042107

Boonstra J, Post JA (2004) Molecular events associated with reactive oxygen species and cell cycle progression in mammalian cells. Gene 337(SUPPL):1–13. https://doi.org/10.1016/j.gene.2004.04.032

Campo A, Samaniego R, Giménez-Abián JF, Giménez-Martín G, López-Sáez JF, Díaz de la Espina SM, De la Torre C (2003) G2 checkpoint targets late replicating DNA. Biol Cell 95(8):521–526. https://doi.org/10.1016/j.biolcel.2003.07.002

Carlson C, Hussein SM, Schrand AM, Braydich-Stolle LK, Hess KL, Jones RL, Schlager JJ (2008) Unique cellular interaction of silver nanoparticles: Size-dependent generation of reactive oxygen species. J Phys Chem B 112(43):13608–13619. https://doi.org/10.1021/jp712087m

Charrad M, Ghazzali N, Boiteau V, Niknafs A (2014) NbClust: an R package for determining the relevant number of clusters in a data set. J Stat Softw 61:1–36

Deepak V, Kalishwaralal K (2011) Metal Nanoparticles in Microbiology. In Metal Nanoparticles in Microbiology (pp. 17–35). https://doi.org/10.1007/978-3-642-18312-6

Dietz KJ, Herth S (2011) Plant nanotoxicology. Trends Plant Sci 16(11):582–589. https://doi.org/10.1016/j.tplants.2011.08.003

Donaldson K, Poland CA, Schins RPF (2010) Possible genotoxic mechanisms of nanoparticles: Criteria for improved test strategies. Nanotoxicology 4(4):414–420. https://doi.org/10.3109/17435390.2010.482751

Durán N, Marcato PD, Durán M, Yadav A, Gade A, Rai M (2011) Mechanistic aspects in the biogenic synthesis of extracellular metal nanoparticles by peptides, bacteria, fungi, and plants. Appl Microbiol Biotechnol 90(5):1609–1624. https://doi.org/10.1007/s00253-011-3249-8

Feizi H, Kamali M, Jafari L, Rezvani Moghaddam P (2013) Phytotoxicity and stimulatory impacts of nanosized and bulk titanium dioxide on fennel (Foeniculum vulgare Mill). Chemosphere 91(4):506–511. https://doi.org/10.1016/j.chemosphere.2012.12.012

Fenech M, Kirsch-Volders M, Natarajan AT, Surralles J, Crott JW, Parry J, Norppa H, Eastmond DA, Tucker JD, Thomas P (2011) Molecular mechanisms of micronucleus, nucleoplasmic bridge and nuclear bud formation in mammalian and human cells. Mutagenesis 26(1):125–132. https://doi.org/10.1093/mutage/geq052

Fernandes TCC, Mazzeo DEC, Marin-Morales MA (2007) Mechanism of micronuclei formation in polyploidizated cells of Allium cepa exposed to trifluralin herbicide. Pestic Biochem Physiol 88(3):252–259. https://doi.org/10.1016/j.pestbp.2006.12.003

Fernández JG, Almeida CA, Fernández-Baldo MA, Felici E, Raba J, Sanz MI (2015) Development of nitrocellulose membrane filters impregnated with different biosynthesized silver nanoparticles applied to water purification. Talanta 146:237–243. https://doi.org/10.1016/j.talanta.2015.08.060

Fernández JG, Fernández-Baldo MA, Berni E, Camí G, Durán N, Raba J, Sanz MI (2016) Production of silver nanoparticles using yeasts and evaluation of their antifungal activity against phytopathogenic fungi. Process Biochem 51(9):1306–1313. https://doi.org/10.1016/j.procbio.2016.05.021

Fiskesjö G (1985) The Allium test as a standard in environmental monitoring. Hereditas 102(1):99–112. https://doi.org/10.1111/j.1601-5223.1985.tb00471.x

Gao D, Zhou H, Wang J, Miao S, Yang F, Wang G, Wang J, Bao X (2015) Size-Dependent Electrocatalytic Reduction of CO2 over Pd Nanoparticles. J Am Chem Soc 137(13):4288–4291. https://doi.org/10.1021/jacs.5b00046

Ghosh Chaudhuri R, Paria S (2012) Core/shell nanoparticles: Classes, properties, synthesis mechanisms, characterization, and applications. Chem Rev 112(4):2373–2433. https://doi.org/10.1021/cr100449n

Gonzalez L, Cundari E, Leyns K-V (2017) Towards a New Paradigm in Nano-Genotoxicology: Facing Complexity of Nanomaterials' Cellular Interactions and Effects. Basic Clin Pharmacol Toxicol 121:23–29. https://doi.org/10.1111/bcpt.12698

Granger CL, Cyr RJ, Mineyuki Y, Anraku Y, Chuong SDX, Park NIl, Freeman MC, Mullen RT, Muench DG, Yoneda A, Akatsuka M, Hoshino H, Kumagai F, Hasezawa S, Sawin KE, Nurse P, Dhonukshe P, Gadella TWJ, Hotta T, Bezanilla M (2004) Cell death by mitotic catastrophe: A molecular definition. J Cell Biol 23(1):10615–10623. https://doi.org/10.1038/sj.emboj.7600916

Grant WF (1982) Chromosome aberration assays in allium: A report of the US environmental protection agency gene-tox program. Mutat Res Genet Toxicol Environ Mutagen 99(3):273–291

Gudikandula K, Vadapally P, Singara Charya MA (2017) Biogenic synthesis of silver nanoparticles from white rot fungi: Their characterization and antibacterial studies. OpenNano 2(June):64–78. https://doi.org/10.1016/j.onano.2017.07.002

Harrison XA (2014) Using observation-level randomeffects to model overdispersion in count data in ecology and evolution. PeerJ *2014*(1). https://doi.org/10.7717/peerj.616

Jaidev LR, Narasimh G (2010) Fungal mediated biosynthesis of silver nanoparticles, characterization and antimicrobial activity. Colloids Surf, B 81(2):430–433. https://doi.org/10.1016/j.colsurfb.2010.07.033

Jeevanandam J, Barhoum A, Chan YS, Dufresne A, Danquah MK (2018) Review on nanoparticles and nanostructured materials: History, sources, toxicity and regulations. Beilstein J Nanotechnol 9(1):1050–1074. https://doi.org/10.3762/bjnano.9.98

Jorge de Souza TA, Rosa Souz LR, Franchi LP (2019) Silver nanoparticles: An integrated view of green synthesis methods, transformation in the environment, and toxicity. Ecotoxicol Environ Saf 171(May 2018):691–700. https://doi.org/10.1016/j.ecoenv.2018.12.095

Kandlikar M, Ramachandran G, Maynard A, Murdock B, Toscano WA (2007) Health risk assessment for nanoparticles: A case for using expert judgment. J Nanopart Res 9(1):137–156. https://doi.org/10.1007/978-1-4020-5859-2_14

Karami MS, De Lima R (2016) Nanoparticles cyto and genotoxicity in plants: Mechanisms and abnormalities. Environ Nanotechnol Monit Manage 6(1):184–193. https://doi.org/10.1016/j.enmm.2016a.08.003

Khan I, Saeed K, Khan I (2019) Nanoparticles: Properties, applications and toxicities. Arab J Chem 12(7):908–931. https://doi.org/10.1016/j.arabjc.2017.05.011

Khoshnamvand M, Huo C, Liu J (2019) Silver nanoparticles synthesized using Allium ampeloprasum L. leaf extract: Characterization and performance in catalytic reduction of 4-nitrophenol and antioxidant activity. J Mol Struct 1175:90–96. https://doi.org/10.1016/j.molstruc.2018.07.089

Kirsch-Volders M, Vanhauwaert A, Eichenlaub-Ritter U, Decordier I (2003) Indirect mechanisms of genotoxicity. Toxicol Lett 140–141:63–74. https://doi.org/10.1016/S0378-4274(02)00498-8

Kumari M, Khan S, Pakrashi S, Mukherjee A, Chandrasekaran N (2011) Cytogenetic and genotoxic effects of zinc oxide nanoparticles on root cells of Allium cepa. J Hazard Mater 190(1–3):613–621. https://doi.org/10.1016/j.jhazmat.2011.03.095

Kumari M, Mukherjee A, Chandrasekaran N (2009) Genotoxicity of silver nanoparticles in Allium cepa. Sci Total Environ 407(19):5243–5246. https://doi.org/10.1016/j.scitotenv.2009.06.024

Kuppusamy P, Yusoff MM, Maniam GP, Govindan N (2016) Biosynthesis of metallic nanoparticles using plant derivatives and their new avenues in pharmacological applications – An updated report. Saudi Pharm J 24(4):473–484. https://doi.org/10.1016/j.jsps.2014.11.013

Laurent A, Nicco C, Chéreau C, Goulvestre C, Alexandre J, Alves A, Lévy E, Goldwasser F, Pani Y, Soubrane O, Weill B, Batteux F (2005) Controlling tumor growth by modulating endogenous production of reactive oxygen species. Can Res 65(3):948–956

Leme DM, Marin-Morales MA (2009) Allium cepa test in environmental monitoring: A review on its application. Mutat Res Rev Mutat Res 682(1):71–81. https://doi.org/10.1016/j.mrrev.2009.06.002

Liu WJ, Qian TT, Jiang H (2014) Bimetallic Fe nanoparticles: Recent advances in synthesis and application in catalytic elimination of environmental pollutants. Chem Eng J 236:448–463. https://doi.org/10.1016/j.cej.2013.10.062

Ma X, Geiser-Lee J, Deng Y, Kolmakov A (2010) Interactions between engineered nanoparticles (ENPs) and plants: Phytotoxicity, uptake and accumulation. Sci Total Environ 408(16):3053–3061. https://doi.org/10.1016/j.scitotenv.2010.03.031

Metz KM, Sanders SE, Pender JP, Dix MR, Hinds DT, Quinn SJ, Ward AD, Duffy P, Cullen RJ, Colavita PE (2015) Green Synthesis of Metal Nanoparticles via Natural Extracts: The Biogenic Nanoparticle Corona and Its Effects on Reactivity. ACS Sustain Chem Eng 3(7):1610–1617. https://doi.org/10.1021/acssuschemeng.5b00304

Mishima M (2017) Chromosomal aberrations, clastogens vs aneugens. Frontiers in Bioscience - Scholar 9(1):1–16. https://doi.org/10.2741/S468

Mohamed AA, Fouda A, Abdel-Rahman MA, Hassan SED, El-Gamal MS, Salem SS, Shaheen TI (2019) Fungal strain impacts the shape, bioactivity and multifunctional properties of green synthesized zinc oxide nanoparticles. Biocatal Agric Biotechnol 19. https://doi.org/10.1016/j.bcab.2019.101103

Mohanta YK, Nayak D, Biswas K, Singdevsachan SK, Abd Allah EF, Hashem A, Alqarawi AA, Yadav D, Mohanta TK (2018) Silver nanoparticles synthesized using wild mushroom show potential antimicrobial activities against food borne pathogens. Molecules 23(3):1–18. https://doi.org/10.3390/molecules23030655

Mukherjee P, Ahmad A, Mandal D, Senapati S, Sainkar SR, Khan MI, Parishcha R, Ajaykumar PV, Alam M, Kumar R, Sastry M (2001) 0152.NanoLett.2001,1,515.pdf

Nagaonkar D, Shende S, Rai M (2015) Biosynthesis of copper nanoparticles and its effect on actively dividing cells of mitosis in Allium cepa. Biotechnol Prog 31(2):557–565. https://doi.org/10.1002/btpr.2040

Ortega FG, Fernández-Baldo MA, Fernández JG, Serrano MJ, Sanz MI, Diaz-Mochón JJ, Lorente JA, Raba J (2015) Study of antitumor activity in breast cell lines using silver nanoparticles produced by yeast. Int J Nanomed 10:2021–2031. https://doi.org/10.2147/IJN.S75835

Pakrashi S, Jain N, Dalai S, Jayakumar J, Chandrasekaran PT, Raichur AM, Chandrasekaran N, Mukherjee A. (2014). In vivo genotoxicity assessment of titanium dioxide nanoparticles by Allium cepa root tip assay at high exposure concentrations. PLoS ONE 9(2). https://doi.org/10.1371/journal.pone.0087789

Park K, Park EJ, Chun IK, Choi K, Lee SH, Yoon J, Le BC (2011) Bioavailability and Toxicokinetics of citrate-coated silver nanoparticles in rats. Arch Pharmacal Res 34(1):153–158. https://doi.org/10.1007/s12272-011-0118-z

Raskar SV, Laware SL (2014) Effect of zinc oxide nanoparticles on cytology and seed germination in onion. Int J Curr Microbiol App Sci 3(2):467–473 (http://www.ijcmas.com/vol-3-2/S.V.RaskarandS.L.Laware.pdf)

Rejeski D (2011) Public Policy on the Technological Frontier. In The Growing Gap Between Emerging Technologies and Legal-Ethical Oversight (pp. 47–59) Springer Dordrech. 7. https://doi.org/10.1007/978-94-007-1356-7

Scherer MD, Sposito JCV, Falco WF, Grisolia AB, Andrade LHC, Lima SM, Machado G, Nascimento VA, Gonçalves DA, Wender H, Oliveira SL, Caires ARL (2019) Cytotoxic and genotoxic effects of silver nanoparticles on meristematic cells of Allium cepa roots: A close analysis of particle size dependence. Sci Total Environ 660:459–467. https://doi.org/10.1016/j.scitotenv.2018.12.444

Schrand AM, Rahman MF, Hussain SM, Schlager JJ, Smith DA, Syed AF (2010) Metal-based nanoparticles and their toxicity assessment. Wiley Interdisciplinary Reviews: Nanomedicine and Nanobiotechnology 2(5):544–568. https://doi.org/10.1002/wnan.103

Shaymurat T, Gu J, Xu C, Yang Z, Zhao Q, Liu Y, Liu Y (2012) Phytotoxic and genotoxic effects of ZnO nanoparticles on garlic (Allium

sativum L.): A morphological study. Nanotoxicology 6(3):241–248. https://doi.org/10.3109/17435390.2011.570462

Siddiqi KS, ur Rahman A, Tajuddin, Husen A (2018) Properties of Zinc Oxide Nanoparticles and Their Activity Against Microbes. Nanoscale Res Lett, 13. https://doi.org/10.1186/s11671-018-2532-3

Singh P, Kim YJ, Zhang D, Yang DC (2016) Biological Synthesis of Nanoparticles from Plants and Microorganisms. Trends Biotechnol 34(7):588–599. https://doi.org/10.1016/j.tibtech.2016.02.006

Singh RP, Ramarao P (2012) Cellular uptake, intracellular trafficking and cytotoxicity of silver nanoparticles. Toxicol Lett 213(2):249–259. https://doi.org/10.1016/j.toxlet.2012.07.009

Zhu H, Han J, Xiao JQ, Jin Y (2008) Uptake, translocation, and accumulation of manufactured iron oxide nanoparticles by pumpkin plants. J Environ Monit 10(6):713–717. https://doi.org/10.1039/b805998e